Journal of Applied Polymer Science

# Synthesis and Characterization of Graft Copolymer of Polyacrylonitrile-*g*-Polyethylene Glycol-Maleic Acid Monoester Macromonomer

**Jing Guo, Piao Xie, Xin Zhang, Chunfang Yu, Fucheng Guan, Yuanfa Liu**
School of Textile and Material Engineering, Dalian Polytechnic University, Dalian 116034, People's Republic of China
Correspondence to: J. Guo (E-mail: guojing8161@163.com)

**ABSTRACT:** A novel solid–solid phase-change energy storage material was synthesized by the aqueous phase precipitation polymerization. The amphiphilic polyethylene glycol-maleic acid monoester macromonomer (MAPEG) with a double bond and a terminal carboxyl was the side chain and the polyacrylonitrile (PAN) was a skeleton. The chemical structure and thermal properties of the graft copolymer were investigated. The results indicated that the MAPEG chains were successfully grafted onto the PAN backbone. The graft copolymer possess good thermal reliability and the phase-transition temperature is in the temperature range of human comfort, meanwhile, the melting enthalpy could reach 74.16 J/g and the crystallization enthalpy could reach 65.40 J/g, accounting for theoretical enthalpy value of 89 and 93%, respectively. Besides, optimum conditions of synthesizing the graft copolymer were determined by orthogonal experiment. © 2013 Wiley Periodicals, Inc. J. Appl. Polym. Sci. **2014**, *131*, 40152.

**KEYWORDS:** copolymers; properties and characterization; thermal properties; grafting; synthesis and processing

Received 30 May 2013; accepted 1 November 2013
**DOI: 10.1002/app.40152**

## INTRODUCTION

With energy and environmental issues becoming increasingly serious, developing new energy sources and improving energy efficiency has become more and more important. Phase-change materials attract the increasing concern and attention[1,2] owing to the advantages of energy storage, heat preservation, and no pollution, which can improve the utilization of energy. The solid–solid phase-change materials have been widely studied[3–5] among all of the phase-change materials. However, the applications of most solid–solid phase-change materials were seriously limited owing to the high phase-transition temperature, low enthalpy, and poor thermal stability. Therefore, developing a novel solid–solid phase-change material has become a common goal.

Polyethylene glycol (PEG) is a valuable phase-change material having a relatively regular chain structure, high crystallinity, and high latent heat of phase change. However, as a solid–liquid phase-change material, PEG has the potential risk of leakage which will be a serious pollution to the environment when the phase transition happens. Therefore, combining PEG with other materials into a solid–solid phase-change materials by blending, graft copolymerization, and other means has become a new research trend.[6–11] For example, PEG10000/poly (glycidyl methacrylate) (PGMA) crosslinked copolymer as a novel solid–solid phase-change material was successfully synthesized through the ring-opening crosslinking reaction of end-carboxyl groups in carboxyl polyethylene glycol and epoxy groups in PGMA.[6] The blends of PEG at average molecular weights of 1000, 6000, and 10,000 g/mol and poly(acrylic acid), or poly(ethylene-*co*-acrylic acid) have been prepared by solution blending and accounted for thermal energy storage properties as solid–solid phase-change material.[7]

In addition, in the past few decades, with the emergence and development of macromonomer method, many new graft copolymers were synthesized using the method as higher grafting rate and the composition of graft copolymer can be controlled by adjusting the proportion of macromonomer and monomer, such as thermosensitive graft copolymer composed of *N*-vinylcaprolactam and poly(ethylene oxide)-alkyl methacrylate macromonomer,[12] gradient graft copolymer derived from two poly(ethylene oxide)-based macromonomers,[13] and other graft copolymers.[14–18] But so far, there were only few reports, which used the macromonomer method for processing PEG and other materials into a solid–solid phase-change material.

In this study, PEG was grafted onto the polyacrylonitrile (PAN) main chain via the intermediate maleic anhydride (MA). The new type of graft copolymer (PAN-*g*-MAPEG) having a solid–solid phase-transition behavior and high phase-change enthalpy was first designed and synthesized by macromonomer method. Besides, optimum conditions of synthesizing PAN-*g*-MAPEG were determined by orthogonal experiment, and the chemical structure and thermal properties of PAN-*g*-MAPEG were analyzed.

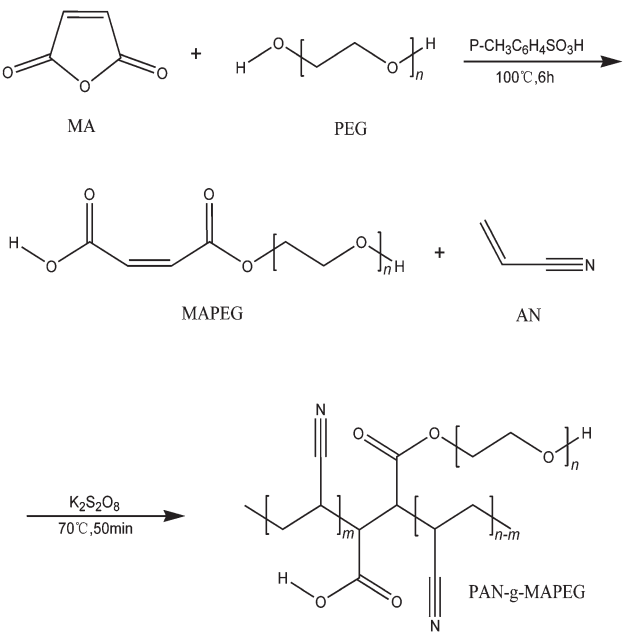


**Figure 1.** Chemical reaction equation of synthetizing the comb graft copolymer PAN-*g*-MAPEG.

## EXPERIMENTAL

### Materials

MA was supplied by Tianjin Bodie Chemicals (Tianjin, China), PEG ($M_n = 4000$) and *P*-toluenesulfonic acid (P-$CH_3C_6H_4SO_3H$) were obtained from Sinopharm Chemicals Reagent (Shanghai, China). Dichloromethane ($CH_2Cl_2$) and anhydrous ethanol ($C_2H_5OH$) were supplied by Tianjin Kermel Chemicals Reagent (Tianjin, China). Ether ($C_4H_{10}O$) was supplied by Tianjin Fuyu Industry of Fine Chemicals (Tianjin, China), acrylonitrile (AN) was obtained from Tianjin Fucheng Chemicals Reagent Factory (Tianjin, China), and potassium persulfate ($K_2S_2O_8$) was supplied by Tianjin East Chemicals Factory (Tianjin, China).

### Synthesis of the PAN-*g*-MAPEG

Solid PEG (MW = 4000) was immersed in an oil bath at 80°C until they turned to colorless solution, and then MA was slowly dropped into the flask with mechanical agitation. After they were compatible with each other, P-$CH_3C_6H_4SO_3H$ used as catalyst in the reaction was added into the flask. As oil bath temperature was elevated to 100°C, the reaction was continued for 6 h at this temperature. After the reaction was completed, the production was filtered and washed twice using dichloromethane and ether, and dried at 40°C in vacuum for 48 h. Then, maleic acid polyethylene glycol monoester (MAPEG) was obtained.

The previously synthesized MAPEG was dissolved in water to prepare the homogeneous solution, and then $K_2S_2O_8$, used as an initiator, was added into the solution. When the oil bath temperature was elevated to the reaction temperature, nitrogen purging system was introduced and AN monomer started to be added dropwise, and reaction monitoring was performed by observing color change of milky. After the reaction, the production was filtered and washed twice using deionized water and anhydrous ethanol, dried at 40°C in vacuum for 48 h, and the graft copolymer PAN-*g*-MAPEG was obtained. The chemical reaction equation is shown in Figure 1.

### Orthogonal Experiment

Four factors and three levels were selected as the inspection object, the selected factors, and levels are listed in Table I.

### Characterization

The structure of the synthesized graft copolymers was characterized using Fourier transform infrared (FTIR), $^1$H-nuclear magnetic resonance ($^1$H-NMR), $^{13}$C-nuclear magnetic resonance ($^{13}$C-NMR), and X-ray diffraction (XRD). The FTIR spectra were recorded within a range of 4500–0 $cm^{-1}$ using a Spectrum One-B FTIR spectrophotometer (PerkinElme, USA). The X-ray diffractogram was measured under a Cu target tube voltage of 40 kV, a tube current of 30 mA, a $2\theta$ range of 1–60°, a scanning speed of 4°/min with a DX-2600 X-ray diffractometer (FangYuan, China). The $^1$H-NMR spectra were recorded using an AV400 spectrometer (Bruker, Switzerland) in deuterated chloroform (dimethyl sulfoxide, DMSO) at room temperature. The $^{13}$C-NMR spectra were recorded by an AV400 spectrometer (Bruker, Switzerland) in DMSO at room temperature.

The thermal properties of the samples were measured by a 200 F3 differential scanning calorimeter (NETZSCH, Germany) which was carried out in $N_2$ atmosphere from 0 to 100°C heated at a rate of 10°C/min.

The thermal stability was studied using a Q50 thermogravimetric analyzer (TA Instruments, USA). The measurements were performed at a temperature range of 0–700°C and a heating rate of 20°C/min under $N_2$ atmosphere.

The thermal conduction was measured by a C-Therm inductor (Catmill, Canada), the initial temperature and the voltage were 20°C and 2405 mV, respectively.

## RESULTS AND DISCUSSION

### Orthogonal Analysis

The results of orthogonal experiment are summarized in Table II, in which the melting enthalpy was used as the experimental index. As summarized in Table II, the initiator content had the greatest impact on the melting enthalpy of PAN-*g*-MAPEG, followed by the mass ratio of AN and MAPEG, but the reaction temperature and reaction time had a less impact.

In addition, optimum conditions of synthesizing PAN-*g*-MAPEG were shown as follows: with the initiator content of

**Table I.** The Four Factors and Three Levels

| | Factors | | | |
|---|---|---|---|---|
| | Mass ratio (AN : MAPEG) | Initiator (%) | Time (min) | Temperature (°C) |
| Level | *A* | *B* | *C* | *D* |
| 1 | 1 : 1 | 0.5 | 30 | 70 |
| 2 | 1 : 1.1 | 1 | 40 | 75 |
| 3 | 1 : 1.2 | 1.5 | 50 | 80 |

**Table II.** The Results of Orthogonal Experiment

| Test numbers | Factors | | | | $\Delta H$, heating (J/g) |
|---|---|---|---|---|---|
| | *A* | *B* | *C* | *D* | |
| 1# | 1 | 1 | 1 | 1 | 57.70 |
| 2# | 1 | 2 | 2 | 2 | 74.16 |
| 3# | 1 | 3 | 3 | 3 | 48.30 |
| 4# | 2 | 1 | 2 | 3 | 63.73 |
| 5# | 2 | 2 | 3 | 1 | 60.40 |
| 6# | 2 | 3 | 1 | 2 | 34.08 |
| 7# | 3 | 1 | 3 | 2 | 41.12 |
| 8# | 3 | 2 | 1 | 3 | 63.61 |
| 9# | 3 | 3 | 2 | 1 | 31.29 |
| I | 60.053 | 54.183 | 51.797 | 49.797 | |
| II | 52.737 | 66.057 | 56.393 | 49.787 | |
| III | 45.340 | 37.890 | 49.940 | 58.547 | |
| R | 14.713 | 28.167 | 6.453 | 8.760 | |

1%, the mass ratio of AN to MAPEG of 1 : 1, the reaction temperature of 80°C, and the reaction time of 40 min.

**Structural Characterization**

Figure 2 shows the FTIR spectra of PAN, MAPEG, and 2# PAN-*g*-MAPEG. As it can be seen from the spectrum of MAPEG, the peak at 1735 $cm^{-1}$ belongs to the stretching vibration peak of the —C═O of MA units and the peak at 1110 $cm^{-1}$ is attributed to the —C—O—C— stretching vibration absorption of PEG units, indicating that MA and PEG were successfully combined into macromonomer MAPEG. Compared with the spectra of PAN and MAPEG, the spectrum of PAN-*g*-MAPEG not only emerges the characteristic peak of —C≡N at 2243 $cm^{-1}$ but also emerges the stretching vibration peak of the —C═O at 1734 $cm^{-1}$ and the stretching vibration peak of the —C—O—C— at 1108 $cm^{-1}$,

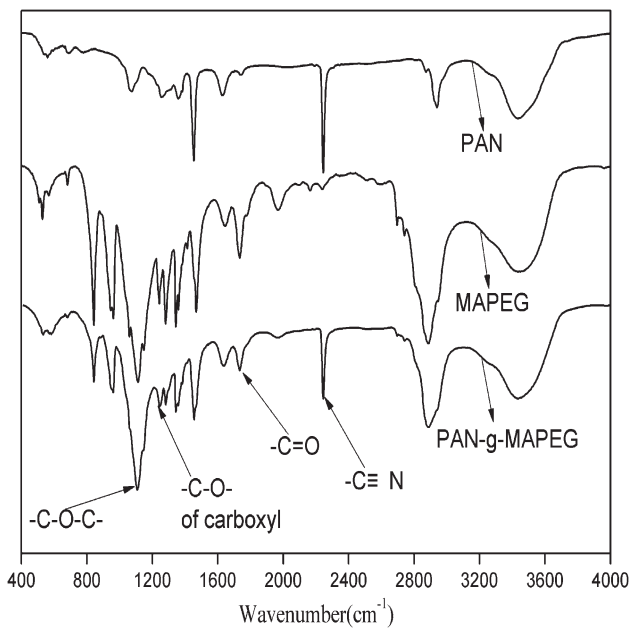


**Figure 2.** FTTR spectra of PAN, MAPEG, and 2# PAN-*g*-MAPEG.

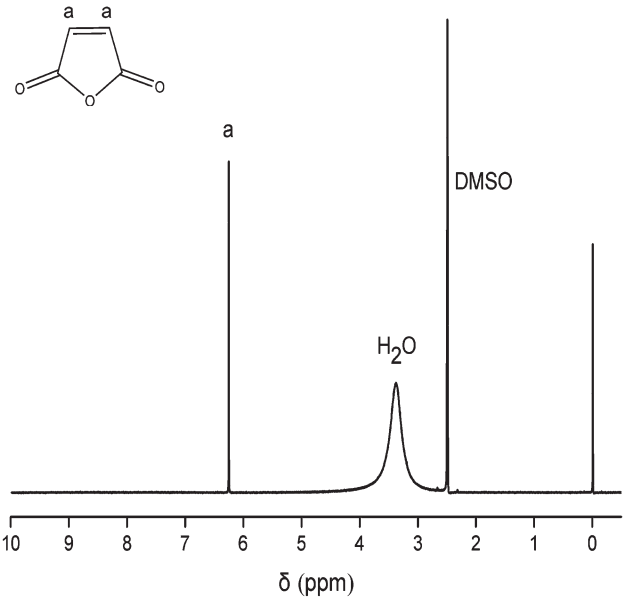


**Figure 3.** $^1$H-NMR spectrum of MA.

indicating that MAPEG was grafted onto PAN chains and the PAN-*g*-MAPEG was obtained successfully.

The $^1$H-NMR spectrum of MA is shown in Figure 3. The peak at $\delta = 6.20$–$6.30$ ppm is the proton signals of the —CH═CH—. Figure 4 shows the $^1$H-NMR spectrum of MAPEG. The chemical shift of the —CH═CH— in MA units is observed in the region $\delta = 6.35$–$6.51$ ppm, and there are two peaks which appear in the region since the presence of cis and trans isomers. The chemical shift of the —$CH_2$— in PEG units appears at $\delta = 3.43$–$3.65$ ppm. The appearance of these two chemical shifts suggests that the macromonomer MAPEG was synthesized successfully.

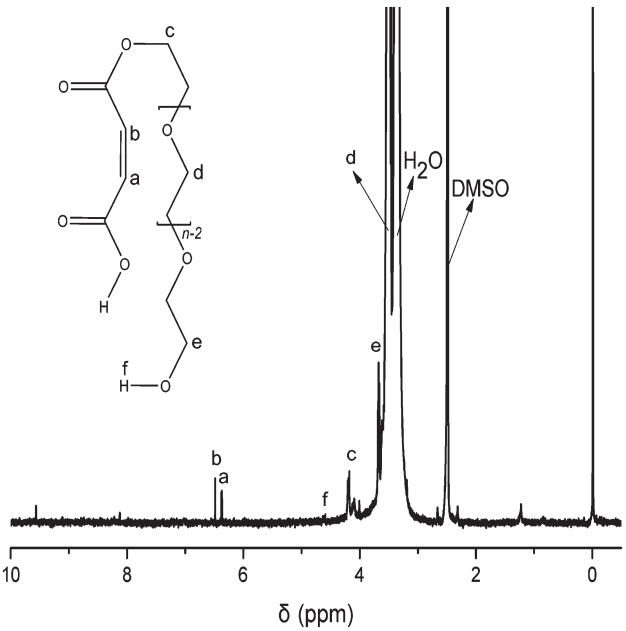


**Figure 4.** $^1$H-NMR spectrum of MAPEG.

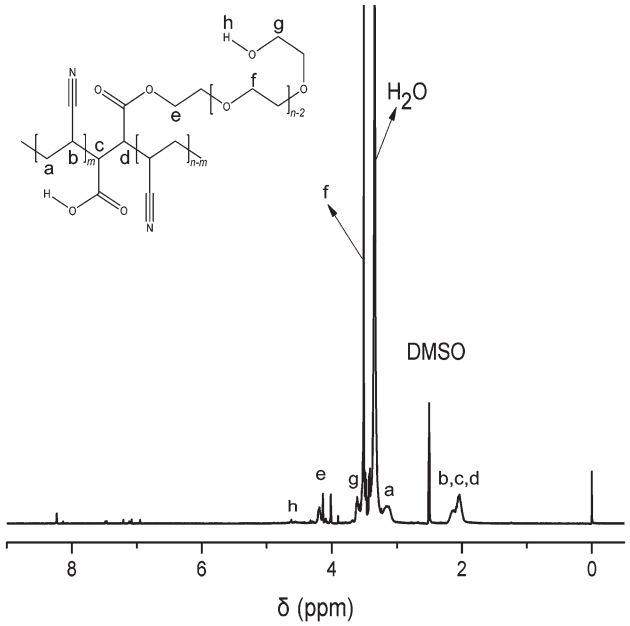


**Figure 5.** $^{1}$H-NMR spectrum of 2# PAN-*g*-MAPEG.

The $^{1}$H-NMR spectrum of 2# PAN-*g*-MAPEG is shown in Figure 5. The peaks are attributed as follows: 3.45–3.56 ppm (—$CH_2$— in MAPEG units), 3.02–3.23 ppm (—$CH_2$— in PAN units), and 1.95–2.23 ppm (—CH—). The appearance of peaks at $\delta = 3.45$–$3.56$ ppm and $\delta = 3.02$–$3.23$ ppm, and the disappearance of peaks at $\delta = 6.35$–$6.51$ ppm indicate that MAPEG was successfully grafted on the PAN. In addition, according to the peak area ratio ($S_a$ : $S_f = 3.23$ : 10.32), the relative mole ratio of AN/MAPEG in the PAN-*g*-MAPEG is 57 : 1.

Figure 6 shows the $^{13}$C-NMR spectrum of 2# PAN-*g*-MAPEG. There are some peaks that appear at $\delta = 26$–$29$ ppm, $\delta = 31$–$34$ ppm,

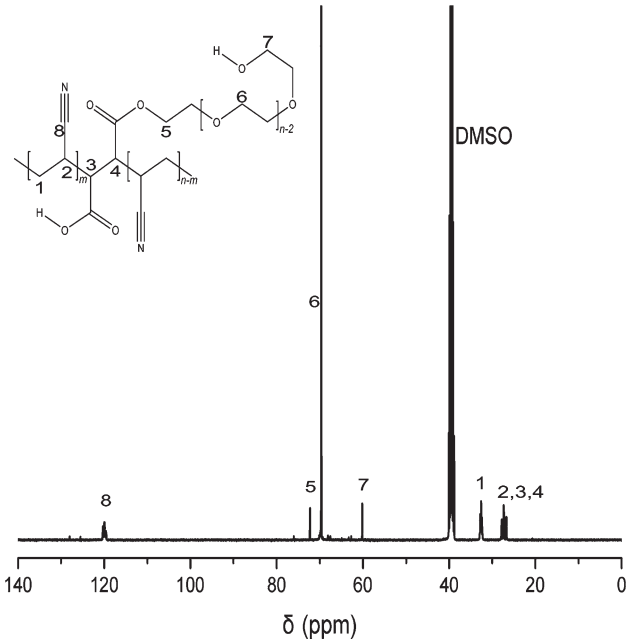


**Figure 6.** $^{13}$C-NMR spectrum of 2# PAN-*g*-MAPEG.

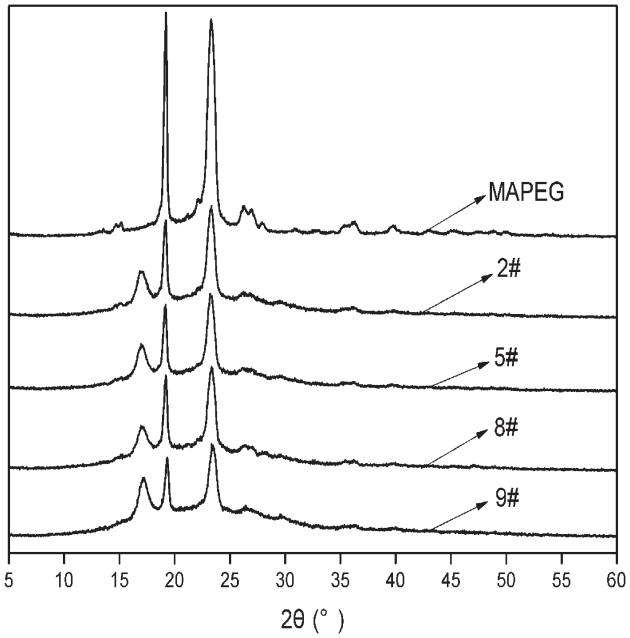


**Figure 7.** XRD patterns of MAPEG and (2#, 5#, 8#, and 9#) PAN-*g*-MAPEG.

$\delta = 119$–$121$ ppm, and $\delta = 70$–$71$ ppm, which represent the chemical shifts of the —CH—, the —$CH_2$— in PAN units, the —C≡N, and the —$CH_2$— in MAPEG units, respectively. The chemical shifts confirm once again that MAPEG was successfully grafted on the PAN.

XRD patterns of MAPEG and (2#, 5#, 8#, and 9#) PAN-*g*-MAPEG are shown in Figure 7. Apparently, there are two very strong diffraction peaks at about 19 and 23° in the pattern of MAPEG. It should be noted that MAPEG had superior crystallization ability and high crystallinity of 94.44% (Table III). As shown in the pattern of PAN-*g*-MAPEG, there are also two peaks at 19 and 23°, and two new diffraction peaks at 17 and 28.9°, which also indicate that MAPEG reacted with AN and the PAN-*g*-MAPEG was obtained successfully. Compared the patterns of (2#, 5#, 8#, and 9#) PAN-*g*-MAPEG, the strength of the main diffraction peaks of the graft copolymers is obviously different when reaction conditions are not the same, and the contributions of the main chains and side chains to the crystallinity of the graft copolymers are also inconsistent. This is because the original crystalline structure of MAPEG was damaged after MAPEG was grafted to PAN main chain, which has a significant impact on the crystallinity of the graft copolymers (Table III).

### Thermal Properties

Figure 8 shows the DSC curves of MAPEG and (2#, 5#, 8#, and 9#) PAN-*g*-MAPEG. Both MAPEG and the graft copolymers

**Table III.** Crystallinity of MAPEG and (2#, 5#, 8#, and 9#) PAN-*g*-MAPEG

| | Samples | | | | |
|---|---|---|---|---|---|
| | MAPEG | 2# | 5# | 8# | 9# |
| Crystallinity (%) | 94.44 | 77.78 | 65.50 | 71.43 | 57.14 |

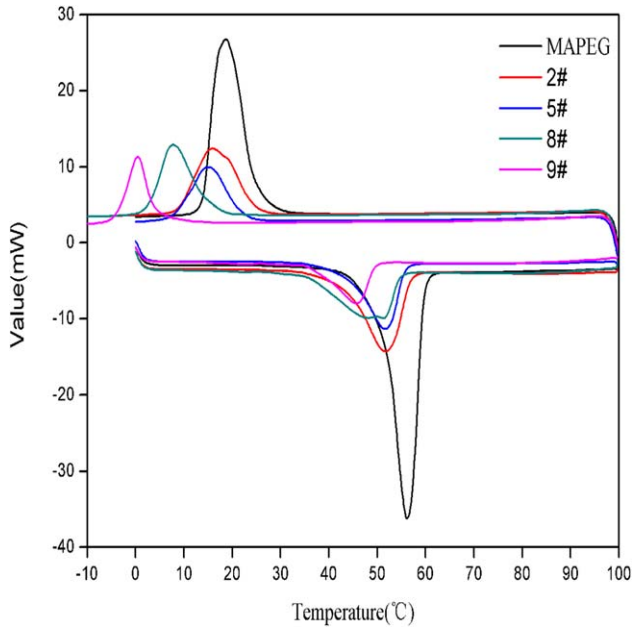


**Figure 8.** DSC curves of MAPEG and (2#, 5#, 8#, and 9#) PAN-*g*-MAPEG. [Color figure can be viewed in the online issue, which is available at wileyonlinelibrary.com.]

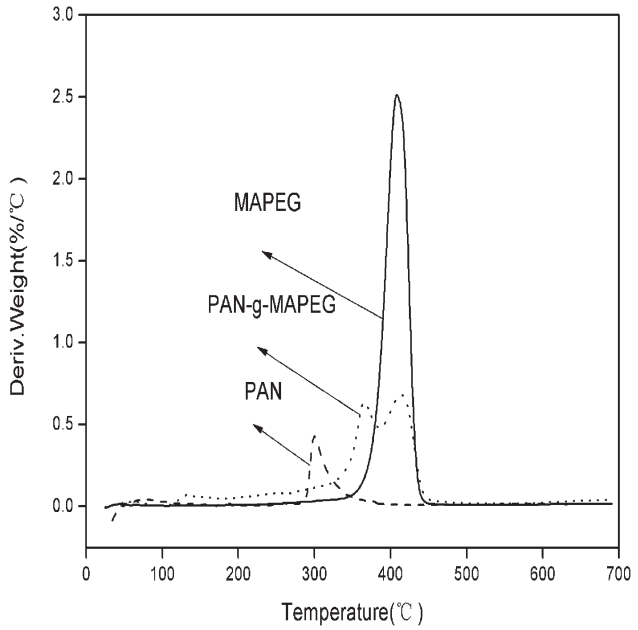


**Figure 9.** TGA curves of PAN, MAPEG, and 2# PAN-*g*-MAPEG.

have an obvious crystallization peak and melting peak, illustrating that they undergone significant phase change. As summarized in Table IV, although the MAPEG shows solid–liquid phase-change behavior, the graft copolymers display solid–solid phase-change behavior which can solve the leakage problem of solid–liquid phase-change material. In addition, the phase-change temperature of the graft copolymers is obviously lower than that of MAPEG. It can be attributed to the fact that just MAPEG side chains play a phase change in the process of phase change of the graft copolymers. After MAPEG was grafted onto PAN, as MAPEG molecular chains were fixed to some degree, the movement ability of MAPEG molecular chains decreased and the crystallization regularity of them was damaged, which lead to the low-phase-change temperature. But the phase-change temperature of the graft copolymers is close to body temperature, and this reflects their great values for people's needs. Based on the data summarized in Table IV, it can also be seen that the melting enthalpy of the graft copolymers could reach 74.16 J/g and the crystallization enthalpy could reach 65.40 J/g, accounting for theoretical enthalpy value of 89 and 93%, respectively (theoretical enthalpy value is half of MAPEG). Moreover, MAPEG>2#>8#>5#>9# (arrange in order of enthalpy), the order is consistent with the crystallinity of them.

The TGA curves of PAN, MAPEG, and 2# PAN-*g*-MAPEG are shown in Figure 9. The initial and the final temperature of thermal decomposition of PAN are approximately at 285 and 350°C, respectively, and its maximum peak of the thermal decomposition emerges at 300°C, whereas the initial and the final temperature of thermal decomposition of MAPEG are at 375 and 425°C, respectively, and its maximum peak of the thermal decomposition emerges at 410°C. However, the initial temperature of thermal decomposition of graft copolymer is at 335°C, compared with the PAN, to higher than 50°C, compared with the MAPEG, to lower than 40°C, indicating that the thermal stability of the graft copolymer is better than the pure PAN, but worse than the MAPEG. In addition, the graft copolymer has two thermal decomposition peaks, because the decompositions of the PAN main chains and the MAPEG side chains did not happen synchronously, and the decomposition of PAN main chains occurred first, and then that of MAPEG side chains after reaching a certain temperature. As shown in Figure 9, it can also be seen that the decomposition of graft copolymer did not occur in the phase-change temperature range, suggesting

**Table IV.** DSC Test Results of MAPEG and (2#, 5#, 8#, and 9#) PAN-*g*-MAPEG

| Samples | $T$, heating (°C) | $T$, cooling (°C) | $T_g$ (°C) | $\Delta H$, heating (J/g) | $\Delta H$, cooling (J/g) | Phase-change behavior |
|---|---|---|---|---|---|---|
| MAPEG | 55.17 | 19.25 | 44 | 166.34 | 140.72 | Solid–liquid |
| 2# | 51.45 | 16.27 | 38 | 74.16 | 65.40 | Solid–solid |
| 5# | 51.36 | 15.21 | 38 | 60.40 | 53.30 | Solid–solid |
| 8# | 51.07 | 8.09 | 35 | 63.61 | 62.93 | Solid–solid |
| 9# | 49.39 | 0.72 | 34 | 31.29 | 39.40 | Solid–solid |

**Table V.** Thermal Conductivity and Endothermic Coefficient of MAPEG and 2# PAN-*g*-MAPEG

| Samples | Thermal conductivity (W/m·K) | Endothermic coefficient ($Ws^{1}/_{2}/m^{2}·K$) |
|---|---|---|
| MAPEG | 0.077 | 159.46 |
| PAN-*g*-MAPEG | 0.066 | 126.26 |

that its thermal stability was good when the phase change happened.

As summarized in Table V, the thermal conductivity and endothermic coefficient of the PAN-*g*-MAPEG copolymer are less than that of the MAPEG. This is because the MAPEG has better crystallinity and hygroscopicity. However, the decrease of the endothermic coefficient of the graft copolymer indicates that its heat transfer capacity declines when it contacts with other materials, which can reduce the impact of external environment on the internal heat of the graft copolymer and improve its heat retaining property.

## CONCLUSIONS

The novel solid–solid phase-change heat storage material (PAN-*g*-MAPEG) was synthesized successfully. The results of FTIR, $^{1}$H-NMR, $^{13}$C-NMR, and XRD confirmed that the MAPEG macromonomer was successfully grafted to the PAN. DSC thermal analyses showed that the melting enthalpy of the graft copolymer could reach 74.16 J/g and the crystallization enthalpy could reach 65.40 J/g, respectively, occupying 89 and 93% of theoretical enthalpy value. The new type of solid–solid phase-change material has a high enthalpy, good thermal stability, and the phase-transition temperature is in the temperature range of human comfort, suggesting that it has broad application prospects.

## ACKNOWLEDGMENTS

The authors appreciate the financial support of the Education Department of General Item of China (LR2012017) and Natural Science Foundation of China (51373027).

## REFERENCES

1. Sharma, A.; Tyagi, V. V.; Chen, C. R.; Buddhi, D. *Renew. Sust. Energy Rev.* **2009**, *13*, 318.
2. Kenisarin, M. M.; Kenisarina, K. M. *Renew. Sust. Energy Rev.* **2012**, *16*, 1999.
3. Sari, A.; Alkan, C.; Bicer, A.; Karaipekli, A. *Sol. Energy Mater. Sol. Cells* **2011**, *95*, 3195.
4. Pielichowska, K.; Pielichowski, K. *Polym. Adv. Technol.* **2011**, *22*, 1633.
5. Shi, H.; Li, J.; Jin, Y.; Yin, Y.; Zhang, X. *Mater. Chem. Phys.* **2011**, *131*, 108.
6. Chen, C.; Liu, W.; Yang, H.; Zhao, Y.; Liu, S. *Sol. Energy* **2011**, *85*, 2679.
7. Alkan, C.; Günther, E.; Hiebler, S.; Himpel, M. *Energy Convers. Manage.* **2012**, *64*, 364.
8. Li, W. D.; Ding, E. Y. *Sol. Energy Mater. Sol. Cells* **2007**, *91*, 764.
9. Li, Y.; Wu, M.; Liu, R.; Huang, Y. *Sol. Energy Mater. Sol. Cells* **2009**, *93*, 1321.
10. Sarı, A.; Alkan, C.; Bicer, A. *Mater. Chem. Phys.* **2012**, *133*, 87.
11. Şentürk, S. B.; Kahraman, D.; Alkan, C.; Gökçe, İ. *Carbohydr. Polym.* **2011**, *84*, 141.
12. Laukkanen, A.; Valtola, L.; Winnik, F. M.; Tenhu, H. *Polymer* **2005**, *46*, 7055.
13. Neugebauer, D.; Zhang, Y.; Pakula, T. *J. Polym. Sci. Polym. Chem.* **2006**, *44*, 1347.
14. Breitenkamp, K.; Simeone, J.; Jin, E.; Emrick, T. *Macromolecules* **2002**, *35*, 9249.
15. Zhang, W.; Shiotsuki, M.; Masuda, T. *Macromolecules* **2007**, *40*, 1421.
16. Zhu, J. L.; Zhang, X. Z.; Cheng, H.; Li, Y. Y.; Cheng, S. X.; Zhuo, R. X. *J. Polym. Sci. Polym. Chem.* **2007**, *45*, 5354.
17. Alshuiref, A. A.; Ibrahim, H. G.; Abduallah, A.; Edali, M. A. *Int. J. Chem.* **2013**, *5*, 58.
18. Zhang, X.; Chen, F.; Zhong, Z.; Zhuo, R. *Macromol. Rapid Commun.* **2010**, *31*, 2155.